

Photocatalytic Degradation of Methylene Blue Dye with Green Synthesized Maghemite Nanoparticles Using Aqueous Extract of *Brassica Tournefortii* Leaves

Wedad Barag*^{ID}, Fatma Shtewi^{ID}, Wedad Al-Adiwish^{ID}, Awatif Tarroush^{ID}

Chemistry Department, Faculty of Science, University of Zawia, 16418, Libya

Corresponding email. w.barag@zu.edu.ly

Abstract

Water pollution has been a major concern for environmentalists worldwide, especially pollution by organic dyes, because dyes are harmful to the environment and ultimately human health. In the present study, *Brassica tournefortii* was first used as a reducing and stabilizing agent via a green approach for the synthesis of maghemite nanoparticles (γ -Fe₂O₃NPs) and evaluated their significant methylene blue dye photocatalytic degradation. The synthesized γ -Fe₂O₃NPs were characterized using UV-Vis, FT-IR, XRD, and SEM techniques. According to UV-Vis spectra, the SPR band at 442 nm with a band gap energy of about 2.65 eV, as well as the surface functional groups of biomolecules, were identified by FT-IR. The XRD confirmed the cubic crystalline structure of γ -Fe₂O₃NPs with a crystallite size of 13.85 nm. While SEM revealed spherical and uniform morphology. The synthesized γ -Fe₂O₃NPs exhibited potential photocatalytic efficiency by degrading 80.12 % of a 10 ppm Methylene blue (MB) dye solution within 90 min under sunlight irradiation, following pseudo second-order kinetic. The presented results revealed that the γ -Fe₂O₃NPs are an attractive photocatalyst for developing effective water purification for organic dyes.

Keywords. *Brassica tournefortii* Leaves Extract, γ -Fe₂O₃NPs, Photocatalytic Degradation, Methylene Blue Dye, Sunlight Irradiation.

Introduction

Iron oxide nanoparticles (IONPs) have attracted much concern owing to their unique properties, such as superparamagnetism, surface-to-volume ratio, greater surface area, a propensity to agglomerate, and easy separation methodology [1]. Iron oxides exist in nature in many forms, which are hematite (α -Fe₂O₃), maghemite (γ -Fe₂O₃), wustite (FeO), and magnetite (Fe₃O₄), being most probably common and important technologically [2]. Among them, maghemite nanoparticles (γ -Fe₂O₃NPs) have attracted particular interest for biomedical applications such as therapeutic and diagnostic applications [2, 3]. Furthermore, maghemite nanoparticles (γ -Fe₂O₃NPs) are an attractive n-type semiconductor with a band gap of 2.0 eV and a spinel structure [4]. Accordingly, it had significant environmental applications such as the removal of heavy metals and photocatalytic degradation of industrial dyes from wastewater [5-7].

To synthesize γ -Fe₂O₃NPs, many methods can be considered, including sonication-calcination method [8], co-precipitation [9], hydrothermal synthesis [10], thermal decomposition [11], and sol-gel method [12]. However, these methods are usually expensive and labor-intensive and are potentially hazardous to the environment and living organisms. Therefore, using the phytochemicals present in plants as bio-reductants is attaining a greater impetus. Various plants have been studied for the green synthesis of γ -Fe₂O₃NPs, such as *Ziziphus jujuba* [7], *Prosopis farcta* [13], *taranjabin* [14], *E. platyloba* [15], and *Phoenix dactylifera* [16]. However, there are no reports on the formation of iron oxide nanoparticles using the *Brassica tournefortii* plant. *Brassica tournefortii* (*B. tournefortii*) is locally known as African mustard or Sahara mustard and belongs to the family Brassicaceae.

Brassica tournefortii is an annual herbaceous plant, native to North Africa and the Middle East [17]. It contains a huge spectrum of various secondary metabolites (glucosinolates, carotenoids, isothiocyanates) and is rich in vitamins and minerals [18]. Recently, the successful green synthesis of silver and copper oxide nanomaterials using *Brassica tournefortii* leaves has been reported. Our research group has synthesized silver nanowires (AgNWs) using an aqueous extract of *Brassica tournefortii* leaves and evaluated their antibacterial and antioxidant activities [19]. Similarly, the green synthesis and antibacterial activity of copper oxide nanoparticles (CuONPs) using an aqueous extract of *Brassica tournefortii* leaves has also been reported [20]. Methylene blue (MB) dye is a cationic organic chloride salt with the cation 3,7 bis(dimethylamino) phenothiazin-5-ium.

Methylene blue dye is recognized as a popular cationic dye utilized in a variety of sectors, including the pharmaceutical, food processing, paint, medicine, and textile industries [5]. Methylene blue dye is harmful to the environment due to its poisonous and carcinogenic properties. The threshold value for methylene blue in the water is about 5–10 mg/L [21], thus requiring the development of an efficient method to reduce organic dyes, include adsorption, chemical precipitation, filtration, ion-exchange, coagulation/flocculation, reverse osmosis, and electro dialysis; unfortunately, these methods have high operating costs and are ineffective in accomplishing the total elimination of organic dyes from wastewater [22]. Photocatalysis is more advantageous than other methods since it remains the most economical, reduces pollution, has no

secondary pollution [7, 22], is eco-friendly, and is widely used. In this study, we successfully synthesized γ -Fe₂O₃ nanoparticles through a rapid, simple, and eco-friendly method, without any hazardous chemicals as reducing or stabilizing agents. The goal of this study has been to synthesize maghemite nanoparticles (γ -Fe₂O₃NPs) using an aqueous extract of *Brassica tournefortii* leaves, and these synthesized γ -Fe₂O₃NPs were employed for the photocatalytic degradation of methylene blue dye under sunlight irradiation.

Experimental Part

materials

Fresh leaves of the *Brassica tournefortii* plant, ferric chloride hexahydrate (FeCl₃ · 6H₂O), sodium hydroxide (NaOH), and methylene blue dye were purchased from Sigma-Aldrich.

Preparation of *Brassica tournefortii* leaves extract

The fresh *Brassica tournefortii* leaves were collected from Zawia city, north Libya. The leaves were thoroughly washed several times using normal water and then followed by distilled water to remove impurities. The (10 g) of leaves were cut into fine pieces and boiled with 100 ml of distilled water for 15 minutes. Then, the extract was filtered through Whatman paper (size No.1). Finally, the aqueous extract was stored at 4°C for future work [19].

Green synthesis of maghemite nanoparticles

For the green synthesis of γ -Fe₂O₃NPs, aqueous extract of *Brassica tournefortii* leaves was added to 0.01M of FeCl₃·6H₂O solution in a 1:1 (v/v) ratio, followed by pH adjustment to 9 by 0.1 M sodium hydroxide solution, and the mixture was stirred for 1 hour at 80°C. The formation of a brown colloidal solution indicates the formation of γ -Fe₂O₃NPs. The colloidal solution was centrifuged at 3000 r/m for 15 minutes to get the powdered nanoparticles, which were washed thoroughly with distilled water and ethanol to remove the unwanted organic matter and air-dried at room temperature for 48 hours. Finally, the γ -Fe₂O₃NPs were calcinated in an electronic oven at 400 °C for 2 hours. The Schematic diagram of the green synthesis of γ -Fe₂O₃NPs is shown in (Figure 1).

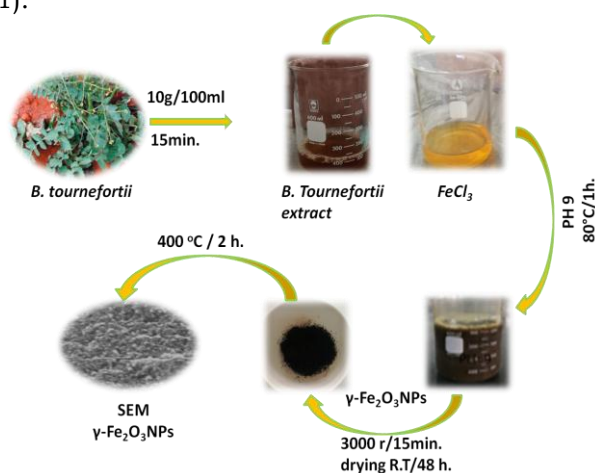


Figure 1. Schematic diagram of γ -Fe₂O₃NP biosynthesized by aqueous *Brassica tournefortii* extract

Chemical characterizations

The optical characteristics of γ -Fe₂O₃NPs were characterized by a UV-vis-NIR spectrometer (Cary Varian 6000i UV-vis), in the range of 200-800 nm. The optical band gap was determined using Touch's plot method $h\nu$ versus $(\alpha h\nu)^{1/2}$, where α and $h\nu$ denote the optical absorption coefficient and photon energy, respectively. The obtained powdered γ -Fe₂O₃NPs were analyzed by FT-IR (IR Affinity-1s (Shimadzu) spectrometer), recorded in the wavenumber range of 500–4,000 cm⁻¹ to find the functional groups present around the synthesized γ -Fe₂O₃NPs. The crystal structure of the sample was analyzed by using XRD (Shimadzu XRD-6100 diffractometer) with a Cu K α radiation monochromatic filter in the range 35–80°. Then, the size of γ -Fe₂O₃NPs was calculated using the Scherrer equation. The morphology of the synthesized γ -Fe₂O₃ NPs was observed by scanning electron microscopy (SEM, LEO 1430VP).

Photocatalytic degradation study

In the photocatalytic degradation study of γ -Fe₂O₃NPs, the methylene blue dye (MB) removal was performed using a 10-ppm methylene blue solution (100 mL) and 50 mg of γ -Fe₂O₃NPs catalyst. The mixtures were kept in dark conditions under stirring and followed with photocatalytic irradiation by sunlight to measure the extent of the dye's adsorption onto the catalyst's surface. The solution was taken every 30 min intervals,

and the absorbance of each methylene blue solution was measured using a UV-Vis spectrophotometer [22]. Similar steps were repeated for all samples. The percent degradation of MB was calculated using Equation (1).

$$\% \text{ Deg.} = [(C_0 - C_t) / C_0] * 100 \quad (1)$$

where % Deg. is the degradation efficiency, C_0 and C_t are defined as the concentration (mg/L) of MB solution before and after sunlight irradiation, respectively. The λ_{max} of the MB solution was recorded to be 664 nm.

Results and Discussion

UV-Vis Spectroscopy analysis

The color change is the preliminary confirmation study for the formation of $\gamma\text{-Fe}_2\text{O}_3\text{NPs}$ biosynthesized by aqueous *Brassica tournefortii* extract. During the reaction, when an aqueous extract of *Brassica tournefortii* leaves was added to an iron chloride solution ($\text{FeCl}_3 \cdot 6\text{H}_2\text{O}$), and the pH was adjusted to 9, the color of the $\text{FeCl}_3 \cdot 6\text{H}_2\text{O}$ solution changed from pale yellow to brown and then to brown black, as shown in (Figure 1). The phytoconstituents of *Brassica tournefortii* leaves extract are sufficient to reduce Fe^{3+} ions to $\gamma\text{-Fe}_2\text{O}_3\text{NPs}$, which act as a reducing and stabilizing agent. The formation and reduction process was monitored by UV-Vis spectrometry. The synthesized $\gamma\text{-Fe}_2\text{O}_3\text{NPs}$ have significant absorption bands between 200 and 800 nm. (Figure 2) UV-Vis spectra showed a broad single absorbance band at 442 nm, corresponding to the characteristic surface plasmon resonance (SPR) of $\gamma\text{-Fe}_2\text{O}_3\text{NPs}$, which is similar to the previous literature [15,16].

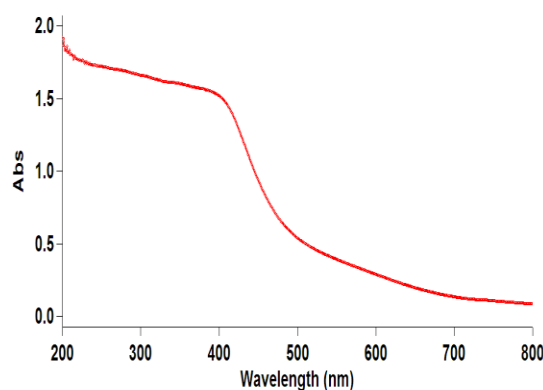


Figure 2. UV-Vis spectra of $\gamma\text{-Fe}_2\text{O}_3\text{NP}$ biosynthesized by aqueous *Brassica tournefortii* extract

The optical band energy of the nano-catalyst is an important factor for photo-catalytic activity. The energy of incident light is provided by a nano-catalyst with a band gap energy equal to or greater than that of the photocatalyst. When enough electrons are stimulated from the valence band (VB) to the conduction band (CB), the photocatalytic behavior of the catalyst will be productive. The band gap (E_g) value of the $\gamma\text{-Fe}_2\text{O}_3\text{NPs}$ has been studied and calculated according to the Tauc equation [23].

$$\alpha h\nu = A(h\nu - E_g)^{0.5} \quad (2)$$

where α is the absorption coefficient, E_g is the band gap energy, A is a constant, and $h\nu$ is the photon energy. Plotting $(\alpha h\nu)^2$ versus $(h\nu)$ plot and linearly regressing the linear portion of the $(\alpha h\nu)^2$ to zero. The optical band gap of synthesized $\gamma\text{-Fe}_2\text{O}_3\text{NPs}$ is shown in (Figure 3). The direct optical band gap of synthesized $\gamma\text{-Fe}_2\text{O}_3\text{NPs}$ has been calculated to be 2.65 eV. This value is lower than the 3.9 eV reported by Priyadarshi et al. [24]. Generally, the band gap of $\text{Fe}_2\text{O}_3\text{NPs}$ ranges widely between 1.8 eV and 3.9 eV. This broad range represents a significant blue shift compared to bulk maghemite (typically around 2.0 eV), which is primarily driven by quantum confinement effects at the nanoscale[4].

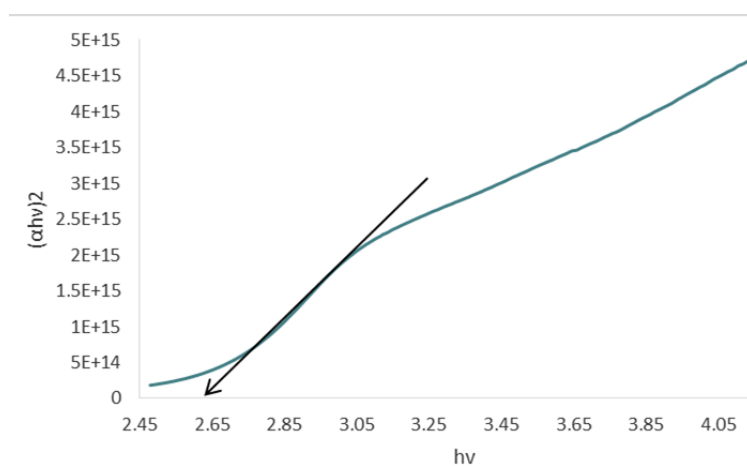


Figure 3. optical band gap energy of γ -Fe₂O₃NP biosynthesized by aqueous *Brassica tournefortii* extract

FT-IR Analysis and Probable Mechanism of γ -Fe₂O₃NP

The FT-IR spectra of *Brassica tournefortii* and γ -Fe₂O₃NPs were investigated in the range 500–4000, as shown in (Figure 4). Characterizing the surface functional groups of γ -Fe₂O₃NPs by FT-IR spectroscopy explains the association of phytochemical components of *Brassica tournefortii* with the γ -Fe₂O₃NPs. As shown in (Figure 4A), a broad absorption band in the region 3100–3300 cm⁻¹ is attributed to the (–OH) stretching vibration of polyphenols and amide (–NH) stretching of the protein component. The peaks at 3027, 2919, and 2850 cm⁻¹ are attributed to the (C–H) stretching of the aromatic ring, asymmetric, and symmetric stretching of aliphatic hydrocarbon, respectively. Moreover, the peak in the range 1736 and 1595 cm⁻¹ shows the presence of (C=O) stretching vibrations and (–C=C–) in the aromatic ring. The peaks at 1428 and 1245 cm⁻¹ correspond to the (C–N) and (O–H) stretching vibrations of polyphenol. The intense peaks at 1143 and 1065 cm⁻¹ depict (C–O) stretching of phenolic compounds.

A band at 838 cm⁻¹ is related to aromatic ring vibration.

The successful capping of the *Brassica tournefortii* onto the surface of γ -Fe₂O₃NPs can be confirmed by FT-IR spectra of γ -Fe₂O₃NPs, presented in (Figure 3B), which reveals the presence of surface O–H groups as indicated by a peak at 3189 cm⁻¹. However, these bands demonstrated shifts and broadening due to overlapping with the O–H stretching band present on the surface of γ -Fe₂O₃NPs. Additionally, the 1557 cm⁻¹ and 1386 cm⁻¹ peaks correspond to C=O and C–O stretching vibrations, respectively, indicating the presence of biomolecules acting as capping agents to stabilize the γ -Fe₂O₃NPs. The maghemite band is observed between 600 and 635 cm⁻¹. Therefore, the Fe–O stretches at 635 cm⁻¹ belong to the maghemite nanoparticles [5,7, 15]. The results of the present study indicated the successful synthesis of γ -Fe₂O₃NPs from *Brassica tournefortii* leaves extract.

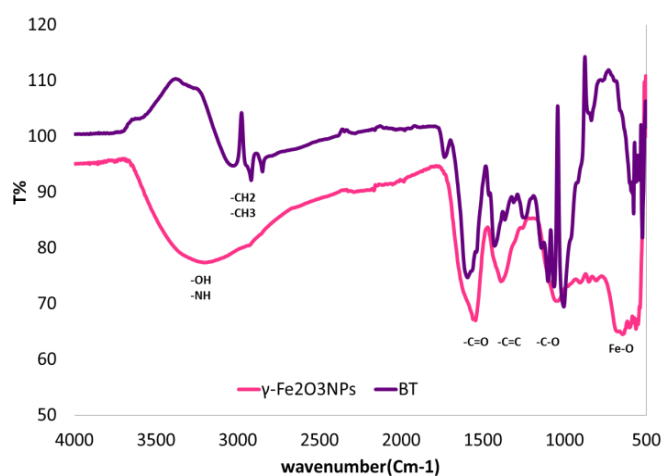
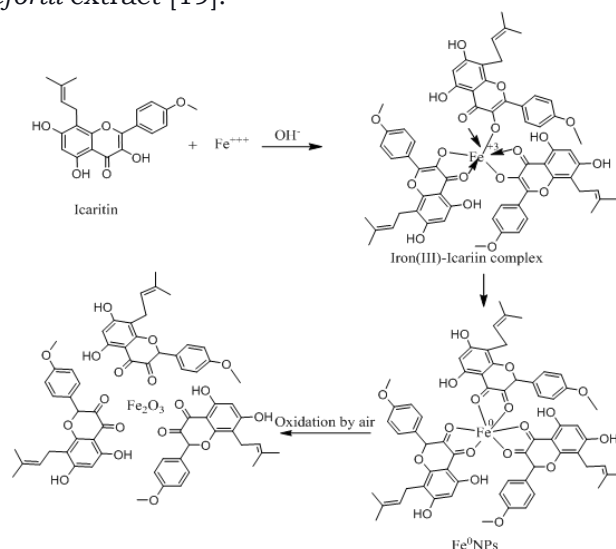


Figure 4. FT-IR spectra of (a) *Brassica tournefortii* leaves and (b) γ -Fe₂O₃NPs

Probable Mechanism of γ -Fe₂O₃ NPs Formation

The exact mechanism of γ -Fe₂O₃NPs remains a challenge. The plausible mechanism of γ -Fe₂O₃NPs biosynthesized by aqueous *Brassica tournefortii* extract is schematically presented in (Scheme 1). Rahmani et al. [18] reported that the leaves of *Brassica tournefortii* are rich in several isothiocyanates and polyphenols,

including icariin, L-tyrosine 7-amido-4-methylcoumarin, Polydatin, 3',5'-dihydroxyflavone, and Phenoxodiol. Among these phytoconstituents, icariin reached the highest concentration with 2.3 mg/g of in the leaves of *Brassica tournefortii*. The phytoconstituents could act as reducing and stabilizing agents for the synthesis of nanoparticles [19]. Accordingly, it is possible that icariin plays the main role in the formation of γ -Fe₂O₃NPs. The icariin will be hydrolyzed to icaritin. Then, the hydroxyl groups of icaritin contained in the extract are deprotonated and are made stronger as a complexing and reducing agent for the iron ions. Subsequently, the Fe³⁺ ions oxidized the hydroxyl groups into carbonyl groups in the reduction reaction as the iron ions were reduced to the zero-valent iron nanoparticles that are oxidized due to the exposure to air, resulting in γ -Fe₂O₃NPs. A similar mechanism was previously reported by our research group for synthesized AgNWs using *Brassica tournefortii* extract [19].



Scheme 1. Plausible mechanism of γ -Fe₂O₃NP biosynthesized by aqueous *Brassica tournefortii* extract

XRD analysis

(Figure 5) shows the X-ray diffraction pattern of γ -Fe₂O₃NP biosynthesized by aqueous *Brassica tournefortii* extract calcinated at 400 °C for 2 hours. The γ -Fe₂O₃NPs exhibited the diffraction peaks at 30.08°, 36.18°, 43.85°, 45.45°, 47.97°, and 63.45°, corresponding to the (220), (311), (400), (422), (511), and (440) for cubic spinal γ -Fe₂O₃NPs powder phase. The resulting peaks and their corresponding Bragg reflections strongly agree with the (JCPDS, file no. 00-039-1346) [25]. From the XRD pattern, it can be observed that some extra diffraction peaks corresponding to α -Fe₂O₃, as reported in previous studies [15,26]. The high peak intensity of (311) at 2 θ =36,18° with narrow full width at half maximum (FWHM) illustrates the good crystalline nature of the synthesized maghemite. The crystallite size of 13.85 nm was estimated by using the Debye-Scherrer equation.

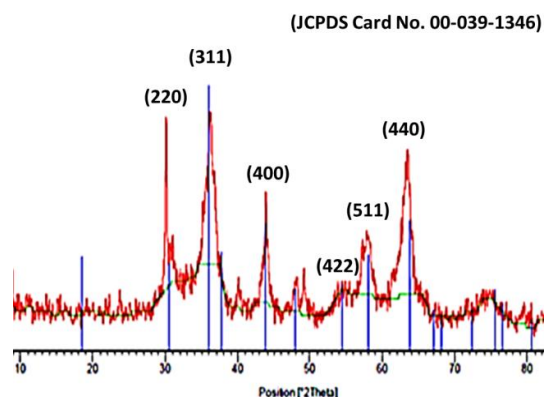


Figure 5. XRD pattern of γ -Fe₂O₃NP biosynthesized by aqueous *Brassica tournefortii* extract

SEM analysis

Scanning electron microscopy (SEM) played a key role in exploring the size and morphology of the nanomaterials because their catalytic and biological behavior strongly depends on size and shape. (Figure 6) shows SEM images of γ -Fe₂O₃NPs biosynthesized by aqueous *Brassica tournefortii* extract. (Figure 6a) shows the SEM image regarding γ -Fe₂O₃NPs, which were air-dried at room temperature for 48 hours and then calcinated in the electronic oven at 400 °C for 2 hours. The SEM image of γ -Fe₂O₃NPs showed that the

majority of the nanoparticles were spherical in shape and uniform in size. The image revealed that the particles were agglomerated, which might be due to the magnetic interactions between the nanoparticles. Similar results have also been reported by Cao et al. [26]. In contrast, (Figure 6 b) illustrates the SEM micrograph of the γ -Fe₂O₃NPs, which was prepared without air-drying at room temperature and then calcinated in the electronic oven at 400 °C for 2 hours. It revealed that the particle size becomes non-uniform, nearly spherical in shape, with agglomeration due to reduced surface free energy.

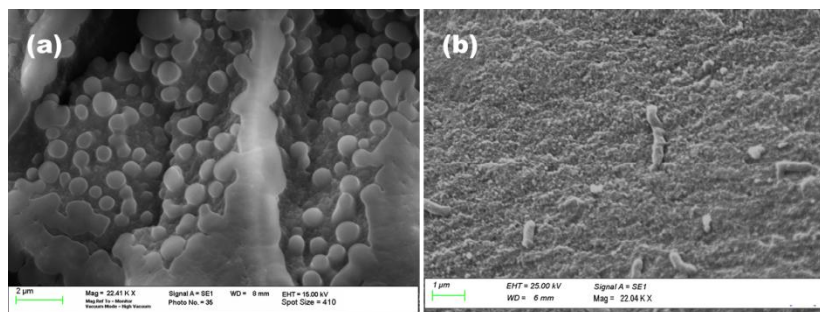


Figure 6. The SEM images of γ -Fe₂O₃NPs biosynthesized by aqueous *Brassica Tournefortii* extract (a), air-dried at r.t (b), without air-drying at r.t.

Photocatalytic Degradation Study

The photocatalytic degradation of MB dye using γ -Fe₂O₃NPs biosynthesized by aqueous *Brassica tournefortii* extract as an efficient photocatalyst is shown in (Figure 7). In order to investigate the photocatalytic activity of γ -Fe₂O₃NPs, the applied test condition included pH = 8, 50 mg of γ -Fe₂O₃NPs, and 10 ppm of MB dye concentration. MB is a synthetic basic dye with sensitive oxidation/reduction properties [5]. The common ionic form is monomeric (MB⁺) in water, which can create dimers and trimers. Two absorbance peaks were observed at 664nm and 292 nm, respectively. The absorbance peak at 664 nm corresponds to (n - π^*) transitions (monomeric (MB⁺) form), which is reduced to dark blue to colourless due to electron transfer. Furthermore, the absorbance peak at 292 nm confirmed the (π - π^*) transitions [27].

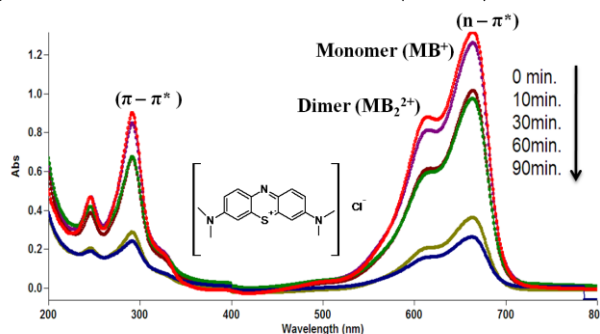


Figure 7. Photocatalytic degradation of MB dye using γ -Fe₂O₃NPs biosynthesized by aqueous *Brassica tournefortii* extract

Figure 8 displays the percentage of degradation of MB dye at different time intervals of the γ -Fe₂O₃NPs. Under dark adsorption, the γ -Fe₂O₃NPs showed removal efficiency at 4.4% within 30 min (before sunlight irradiation). The removal efficiency was further enhanced to reach 80.12 % within 90 min under sunlight irradiation. Miri et al. [7] observed that the synthesized γ -Fe₂O₃NPs NPs using aqueous extract of *Ziziphus jujube* degraded about 92.8% of methylene blue dye during 160 minutes under sunlight irradiation.

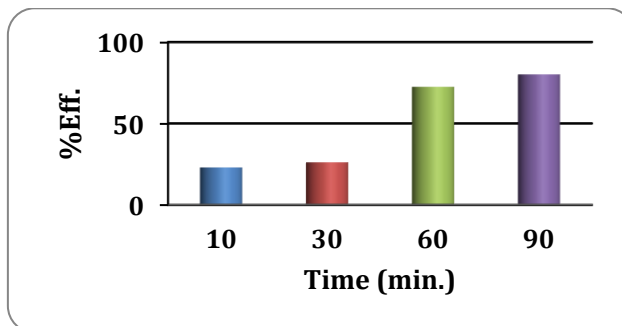


Figure 8. The percentage of degradation of MB dye at different time intervals of γ -Fe₂O₃NPs biosynthesized by aqueous *Brassica tournefortii* extract

The kinetic experiment for MB dye degradation was carried out under optimized conditions using the absorbance of the dye solution measured at 0, 10, 30, 60, and 90 min. The kinetics of methylene blue adsorption on $\gamma\text{-Fe}_2\text{O}_3\text{NPs}$ was evaluated using the pseudo-first-order Equation (3) and the pseudo-second-order Equation (4).

$$\ln(q_e - q_t) = \ln q_e - k_1 t \quad (3)$$

$$t/q_t = \frac{1}{k_2(q_e)^2} + \frac{t}{q_e k_2(q_e)^2} + \frac{t}{q_e} \quad (4)$$

where k_1 (min^{-1}) and k_2 are the rates of sorption ($\text{g.mg}^{-1}\text{min}^{-1}$), q_e is the amount of methylene blue removed at equilibrium (mg.g^{-1}), and q_t is the amount of methylene blue removed at t time (mg.g^{-1}). (Figure 9 and Table 1) showed that $\gamma\text{-Fe}_2\text{O}_3\text{NPs}$ biosynthesized by aqueous *Brassica tournefortii* extract followed the pseudo-second model rather than the pseudo-first-order model.

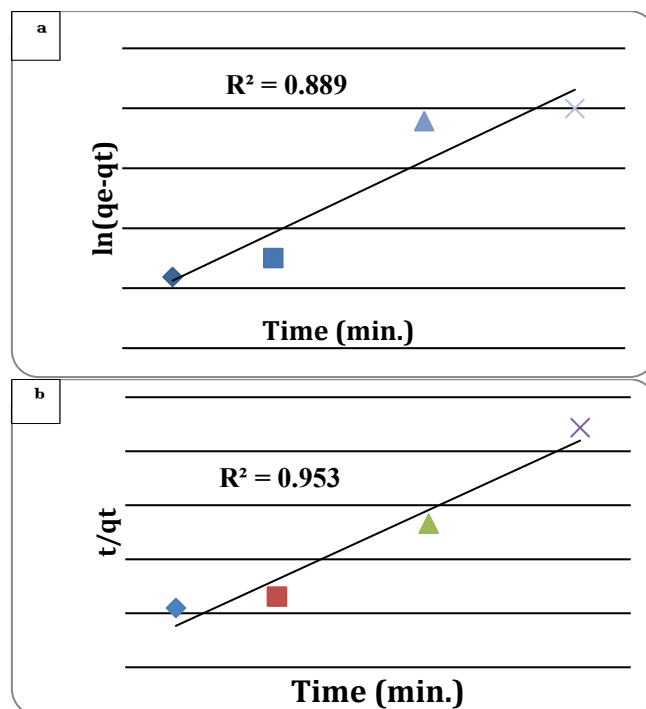


Figure 9. a) Pseudo first-order kinetic b) Pseudo second-order kinetic for photocatalytic degradation of MB dye using $\gamma\text{-Fe}_2\text{O}_3\text{NPs}$ biosynthesized by aqueous *Brassica tournefortii* extract

Table 1. Data of the kinetics model of pseudo-first order and second order for $\gamma\text{-Fe}_2\text{O}_3\text{NPs}$ biosynthesized by aqueous *Brassica tournefortii* extract

	pseudo-first order	pseudo-second order
K	0.019	4.289
R²	0.889	0.953

Proposed mechanism of MB dye photocatalytic degradation

(Figure 10) shows the proposed mechanism of MB dye photocatalytic degradation using $\gamma\text{-Fe}_2\text{O}_3\text{NPs}$ biosynthesized by aqueous *Brassica tournefortii* extract. During degradation, when excited by sunlight, $\gamma\text{-Fe}_2\text{O}_3\text{NPs}$ generate electron-hole pairs on the surface of the $\gamma\text{-Fe}_2\text{O}_3\text{NPs}$ at a band gap of 2.65 eV; both hydroxyl radicals (HO^\bullet) and superoxide anion radicals ($\text{O}_2^{\bullet-}$) are formed by the reaction of charge carriers (e^-/h^+ pairs) with H_2O and O_2 . The hydroxyl radicals play an important role in the degradation of methylene blue dye [28]. These free radicals of high reactivity and high oxidation potential may react with methylene blue dye, converting it into nontoxic products such as degraded compounds, carbon dioxide, and water [29], as shown in the following series of the following reactions:

- $\gamma\text{-Fe}_2\text{O}_3\text{ NPs} + h\nu \rightarrow \gamma\text{-Fe}_2\text{O}_3\text{ NPs} (e^- + h^+)$
- $\text{H}_2\text{O}/\text{OH}^- + \gamma\text{-Fe}_2\text{O}_3\text{ NPs} (h^+) \rightarrow \text{OH}^\bullet + \text{H}^+ + \gamma\text{-Fe}_2\text{O}_3\text{ NPs}$
- $\gamma\text{-Fe}_2\text{O}_3\text{NPs} (e^-) + \text{O}_2 \rightarrow \text{O}_2^{\bullet-} + \text{H}^+$
- $\text{O}_2^{\bullet-} + \text{H}^+ \rightarrow \text{HO}_2^\bullet$
- $2 \text{HO}_2^\bullet \rightarrow \text{H}_2\text{O}_2 + \text{O}_2$

- $\text{H}_2\text{O}_2 \rightarrow \text{OH}^\cdot + \text{OH}^\cdot$
- $\text{H}_2\text{O}_2 + \gamma\text{-Fe}_2\text{O}_3 \text{ NPs } (e^-) \rightarrow \text{OH}^\cdot + \text{OH}^- + \gamma\text{-Fe}_2\text{O}_3 \text{ NPs}$

The MB dye molecules absorb energy and are excited by transferring electrons to produce Fe^{2+} , as shown in the following reaction [28,30]:

- $\text{MB Dye} + h\nu \rightarrow \text{MB}^\cdot\text{Dye}$
- $\text{MB}^\cdot\text{Dye} + \gamma\text{-Fe}_2\text{O}_3 \text{ NPs} \rightarrow \gamma\text{-Fe}_2\text{O}_3 \text{ NPs} + \text{MB Dye}^{e+}$
- $\text{OH}^\cdot + \text{MB}^\cdot\text{Dye}^{e+} \rightarrow \text{Degradation product} + \text{CO}_2 + \text{H}_2\text{O}$

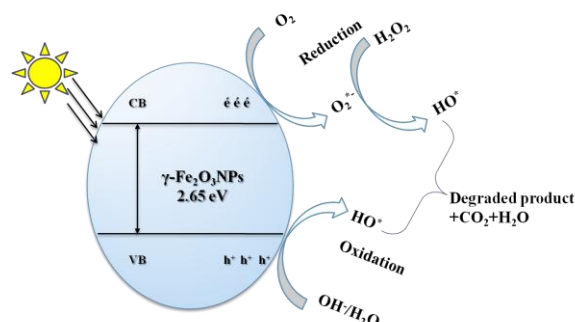


Figure 10. Proposed mechanism for photodegradation of MB using $\gamma\text{-Fe}_2\text{O}_3$ NPs biosynthesized by aqueous *Brassica tournefortii* extract

Conclusion

From the results, it can be concluded that an eco-friendly, efficient, and nontoxic method was used to synthesize maghemite nanoparticles using aqueous ferric chloride solution as precursor and the aqueous extract of *Brassica tournefortii* leaves as a reducing and stabilizing agent. The synthesized $\gamma\text{-Fe}_2\text{O}_3$ NPs optical, structural, and morphological characteristics were investigated using UV-Vis, FTIR, XRD, and SEM techniques. The synthesized $\gamma\text{-Fe}_2\text{O}_3$ NPs exhibited potential photocatalytic activity towards the degradation of methylene blue dye on exposing to sunlight irradiation. The degradation effectiveness against the methylene blue dye was found to be 80.12% within 90 min. Based on the findings of this study, the $\gamma\text{-Fe}_2\text{O}_3$ NPs biosynthesized by aqueous *Brassica tournefortii* extract can be used as an efficient photocatalyst for water treatment technology.

Abbreviations

$\gamma\text{-Fe}_2\text{O}_3$ NPs: maghemite nanoparticles
 SPR: Surface plasmon resonance
 FT-IR: Fourier transform infrared spectroscopy
 UV-Vis: Ultraviolet-visible spectroscopy
 XRD: X-ray diffraction analysis
 SEM: Scanning electron microscopy
 MB dye: Methylene blue dye

Author Contributions

All authors contributed to the study conception and design. Material preparation, data collection, and analysis were performed by Barag W.M., Shtewi F. A., Tarroush A.A.U., and Al-Adiwish W.M. The first draft of the manuscript was written by Barag W.M. and Shtewi F. A. All authors have read and agreed to the published version of the manuscript.

Conflict Of Interests

The authors declare that they have no conflict of interest.

Acknowledgments

The authors are grateful to the Department of Chemistry at Zawia University and the Libyan Medical Research Center in Zawia for providing lab facilities and equipment to perform this study. Petroleum Training & Qualifying Institute in Tripoli for providing the XRD & SEM, and Polymer Research Center in Tripoli for providing FT-IR.

References

1. Ajinkya N, Yu X, Kaithal P, Luo H, Somani P, Ramakrishna S. Magnetic Iron Oxide Nanoparticle (IONP) Synthesis to Applications: Present and Future. *Materials*. 2020 Oct 15;13(20):4644. doi: 10.3390/ma13204644.

2. Shoudho KN, Uddin S, Rumon MMH, Shakil MS. Influence of Physicochemical Properties of Iron Oxide Nanoparticles on Their Antibacterial Activity. *ACS Omega*. 2024 Aug 15;9(33):33303-33334. doi: 10.1021/acsomega.4c02822.
3. Zúñiga-Miranda J, Guerra J, Mueller A, Mayorga-Ramos A, Carrera-Pacheco SE, Barba-Ostria C, et al. Iron Oxide Nanoparticles: Green Synthesis and Their Antimicrobial Activity. *Nanomaterials*. 2023 Nov 17;13(22):2919. doi: 10.3390/nano13222919.
4. Yousif NA, Al-Jawad SMH, Taha AA, Stamatias H. A Review of Structure, Properties, and Chemical Synthesis of Magnetite Nanoparticles. *J Appl Sci Nanotechnol*. 2023 Mar 11;3(1):18-31. doi: 10.53293/jasn.2022.5179.1178.
5. Thakur R, Kaur N, Kaur M, Bhowmik PK, Han H, Singh K, et al. Green Synthesis of Magnetic Fe₂O₃ Nanoparticle with *Chenopodium glaucum* L. as Recyclable Heterogeneous Catalyst for One-Pot Reactions and Heavy Metal Adsorption. *Molecules*. 2024 Oct 3;29(19):4583. doi: 10.3390/molecules29194583.
6. Doan L. Modifying Superparamagnetic Iron Oxide Nanoparticles as Methylene Blue Adsorbents: A Review. *Chem Engineering*. 2023 Aug 21;7(5):77. doi: 10.3390/chemengineering7050077.
7. Miri A, Sedighi AS, Najafidoust A, Khatami M, sarani M. Study of photodegradation performance and ability of lead removal of green synthesized maghemite nanoparticles Using *Ziziphus Jujuba* Extract. *Int J Environ Anal Chem*. 2023;103(19):8369-8383. doi: 10.21203/rs.3.rs-545585/v1.
8. Khoiroh LM, Khidin F, Ningsih R. Synthesis of Maghemite (γ -Fe₂O₃) nanoparticles pigment from lathe waste by sonication – calcination method. *IOP Conf Ser Earth Environ Sci*. 2020;456:012005. doi:10.1088/1755-1315/456/1/012005.
9. Tabassum N, Singh V, Chaturvedi VK, Vamanu E, Singh MP. A Facile Synthesis of Flower-like Iron Oxide Nanoparticles and Its Efficacy Measurements for Antibacterial, Cytotoxicity and Antioxidant Activity. *Pharmaceutics*. 2023 Jun 1;15(6):1726. doi: 10.3390/pharmaceutics15061726.
10. Sreeja V, Joy PA. Microwave-hydrothermal synthesis of γ -Fe₂O₃ nanoparticles and their magnetic properties. *Mater Res Bull*. 2007 Aug 31;42(8):1570-1576. doi: 10.1016/j.materresbull.2006.11.004.
11. Zhou W, Tang K, Zeng S, Qi Y. Room temperature synthesis of rod-like FeC₂O₄·2H₂O and its transition to maghemite, magnetite and hematite nanorods through controlled thermal decomposition. *Nanotechnology*. 2008 Jan 18;19(6):065602. doi: 10.1088/0957-4484/19/6/065602.
12. Parhizkar J, Habibi MH. Synthesis, characterization and photocatalytic properties of Iron oxide nanoparticles synthesized by sol-gel autocombustion with ultrasonic irradiation. *Nanochem Res*. 2017;2(2):166-171. doi: 10.22036/ncr.2017.02.006.
13. Akbarizadeh MR, Naderifar M, Mousazadeh F, et al. Cytotoxic activity and Magnetic Behavior of green synthesized iron oxide nanoparticles on brain glioblastoma cells. *Nanomed Res J*. 2022;7(1):99-106. doi: 10.22034/nmrj.2022.01.010.
14. Miri A, Najafzadeh H, Darroudi M, et al. Iron oxide nanoparticles: biosynthesis, magnetic behavior, cytotoxic effect. *ChemistryOpen*. 2021;10(3):327-333. doi: 10.1080/16583655.2024.2357820.
15. Shahabadi N, Zendejsheshm S, Jamshidi D, Khademi F, Soltani L. Green synthesis of γ -Fe₂O₃@SiO₂ magnetic nanoparticles functionalized with penciclovir drug: antiproliferative effect, and nucleic acids (DNA and RNA) interaction. *J Taibah Univ Sci*. 2024 Dec 31;18(1):2357820. doi: 10.1080/16583655.2024.2357820.
16. Abdullah JAA, Eddine LS, Abderrhmane B, et al. Green synthesis and characterization of iron oxide nanoparticles by phoenix dactylifera leaf extract and evaluation of their antioxidant activity. *Sustain Chem Pharm*. 2020 Sep;17:100280. doi: 10.1016/j.scp.2020.100280.
17. Rahmani R, Beaufort S, Villarreal Soto AS, Taillandier P, Bouajila J, Debouba M. Kombucha fermentation of African mustard (*Brassica tournefortii*) leaves: Chemical composition and bioactivity. *Food Biosci*. 2019 Aug;30:100414. doi: 10.1016/j.fbio.2019.100414.
18. Rahmani R, Bouajila J, Jouaidi M, Debouba M. African mustard (*Brassica tournefortii*) as source of nutrients and nutraceuticals properties. *J Food Sci*. 2020 Jun;85(6):1856-1871. doi: 10.1111/1750-3841.15157.
19. Barag WM, Shtewi FA, Tarroush AAU, Al-Adiwish WM, Altounsi MK. Green Synthesis of Silver Nanowires Using *Brassica Tournfortii* Leaves Extract and Evaluation of Their Antibacterial and antioxidant Activities. *J Appl Organomet Chem*. 2025;5(1):13-27. doi: 10.48309/JAOC.2025.485302.1244.
20. Barag WM, Shtewi FA, Al-Adiwish WM, Tarroush AAU. First Report of green Synthesis of Copper Oxide Nanoparticles from *Brassica Tournfortii* Leaves Extract and Their Antibacterial Activity. *Libyan J Med Res*. 2023;16(2B):60-73. doi: 10.54361/ljmr.16B206,2023.
21. Khan I, Saeed K, Zekker I, Zhang B, Hendi AH, Ahmad A, et al. Review on Methylene Blue: Its Properties, Uses, Toxicity and Photodegradation. *Water*. 2022 Jan 12;14(2):242. doi:10.3390/w14020242.
22. Rathi VH, Jeice AR. Green fabrication of nanoparticles using various plant extracts and their multifaceted applications in photocatalytic cationic dye degradation and antimicrobial activities. *Biomass Convers Biorefin*. 2023 Apr 24. doi:10.1007/s13399-023-04350-2.
23. Mott NF, Davis EA. *Electronic Processes in Non-Crystalline Materials*. 2nd ed. Oxford: Clarendon Press; 1979.
24. Priyadarshi H, Singh K, Shrivastava A. Experimental study of maghemite nanoparticles towards sustainable energy storage device application. *Mater Sci Semicond Process*. 2022 Aug;147:106698. doi:10.1016/j.mssp.2022.106698.
25. Joint Committee on Powder Diffraction Standards (JCPDS). Cards: FeO [6–711], α -Fe₂O₃ [16–653], Fe₃O₄ [19–629], γ -Fe₂O₃ [39–1346]. Swarthmore, PA: JCPDS; [year unknown].
26. Cao D, Li H, Pan L, Li J, Wang X, Jing P, et al. High saturation magnetization of γ -Fe₂O₃ nano-particles by a facile one-step synthesis approach. *Sci Rep*. 2016 Aug 19;6:32360. doi: 10.1038/srep32360.
27. Zubrik A, Jáger D, Mačingová E, Matik M, Hrdzák S. Spontaneous degradation of methylene blue adsorbed on magnetic biochars. *Sci Rep*. 2023 Sep 6;13:14773. doi:10.1038/s41598-023-39976-9.

28. Liang C, Liu H, Zhou J, Peng X, Zhang H. One-Step Synthesis of Spherical γ -Fe₂O₃ Nanopowders and the Evaluation of Their Photocatalytic Activity for Orange I Degradation. *J Chem.* 2015;2015:791829. doi:10.1155/2015/791829.
29. Riyanti F, Hasanudin H, Rachmat A, Purwaningrum W, Hariani PL. Photocatalytic degradation of methylene blue and Congo red dyes from aqueous solutions by bentonite-Fe₃O₄ magnetic. *Commun Sci Technol.* 2023;8(1):1-9. doi:10.21924/cst.8.1.2023.1007.
30. Boddu S, Marri BP, Katika RM, Mikkili I, Dulla JB, Allugunulla VN, et al. Green Synthesis of Copper Oxide Nanoparticles (CuONPs) using Ricinus Communis: Efficient Photocatalytic Dye Degradation and Antibacterial Applications. *Water Air Soil Pollut.* 2025;236(3):209. doi:10.1007/s11270-025-07841-2.